

Pit Propagation Measurements in Experimental 6XXX Alloys

B.A. Shaw, M.M. McCosby, E.Sikora, A. Shi, and H.W. Pickering
Penn State University
University Park, PA 16802

Pit propagation rate experiments and electron microscopy studies were conducted in order to gain insight into the mechanisms responsible for pitting and intergranular corrosion of three experimental Al 6XXX alloys. The alloys were similar to Al 6013 and Al 6111 and contained 0.76-0.78 Si, 0.24-0.25 Fe, 0.59-0.62 Mg with varying Cu additions - Al 6XXX (with no added Cu), Al-6XXX (with 0.68% Cu added), and Al-6XXX (with 1.47% Cu added). The pit propagation rate experiments utilized specimens where the entire polarized specimen functioned as an artificial pit and optical video monitoring of dissolution of the corroding pit bottom was conducted as a function of time. The electrolyte in these experiments was 0.05M HCl and the artificial pits were polarized at a potential of either -300 mV_{SCE} or 0 mV_{SCE} for a period of several days.

Pit propagation rate experiments on the Cu-containing Al 6XXX alloys (at applied potentials of -300 mV_{SCE} and 0 mV_{SCE}) in 0.05 M HCl revealed significant intergranular corrosion (IGC) of the artificial pit bottom with substantial hydrogen gas evolution within the intergranular grooves. Without added Cu, the corrosive attack within the occluded cell was more uniform with substantial sub-grain (localized crystalline) attack of the alloy (possibly associated with the Mg₂Si precipitates in the microstructure). However, transitions between intergranular and uniform attack were observed for the non Cu-containing alloy. With increasing Cu concentration, the degree of sub-grain attack diminished and the degree of IGC

increased. The increase in IGC with increasing Cu is presented in Figures 1 and 2. The reduction in subgrain attack with increasing Cu concentration is also illustrated in Figure 2. The band of intergranular attack under these highly polarized conditions ($E = -0.3V_{SCE}$) penetrated 1 to 2 mm into the alloy (after several days of polarization) and a large number of detached grains were noticed within the confines of the artificial pit. A plot of the thickness of the IGC band versus copper concentration in the alloys is presented in Figure 3 and reveals an increasing band of IGC with increasing Cu content in the alloy. Transitions between intergranular and uniform attack of the artificial pit bottom were observed for the non Cu-containing alloy and are reflected in the wide error bands noted for this alloy. In open-circuit corrosion potential measurements, IGC was noted for the Cu-containing Al 6XXX alloys exposed to chloride-containing environments; however, penetration depths were much lower.

Pitting propagation studies for the three 6XXX alloys indicated some degree of intergranular corrosion of the artificial pit bottom for each of the alloys with the amount of intergranular corrosion increasing and the amount of subgrain attack decreasing as the Cu concentration in the alloy increases. The implications of these findings on the mechanism of pitting corrosion in the three alloys will be explored .

Acknowledgement

This work was sponsored by ALCOA..

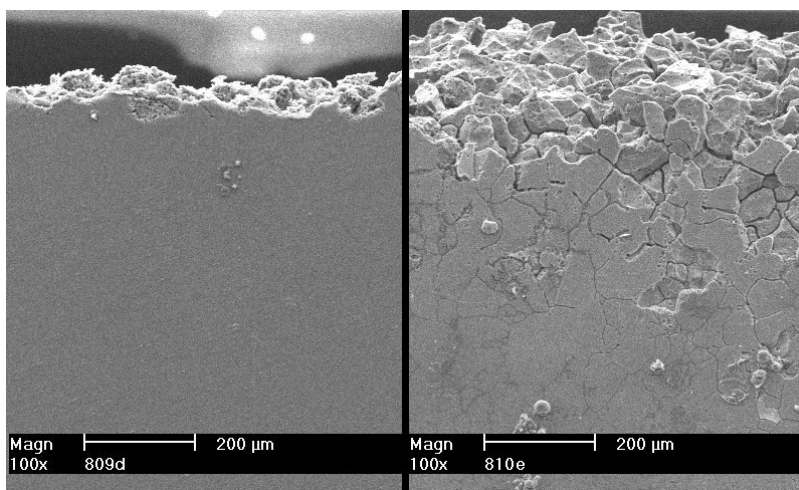


Figure 1. SEM micrographs after polarization for 9 days at $-300 \text{ mV}_{\text{SCE}}$ illustrating the differences between (left) the uniform dissolution of the Al 6XXX alloy and (right) the dominant intergranular attack in the Al 6XXX alloy containing 1.47% Cu.

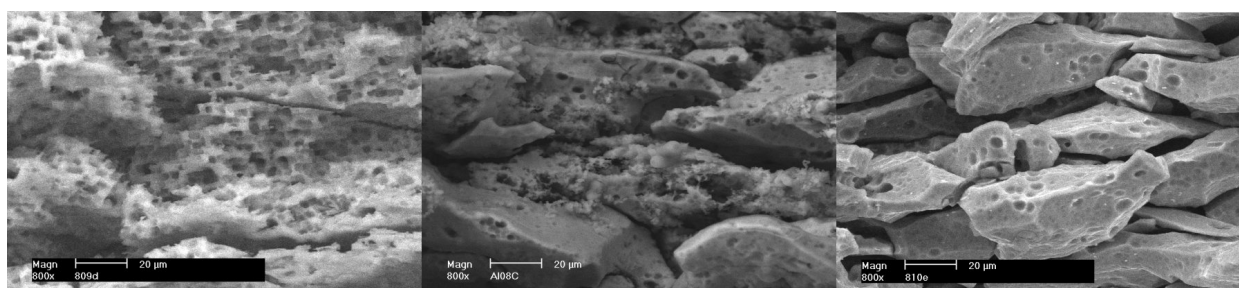


Figure 2 SEM Micrograph showing the degree of subgrain and intergranular attack for the Al6XXX alloys with and without Cu: (left) 0% Cu, (middle) 0.68%Cu, and (right) 1.47% Cu.

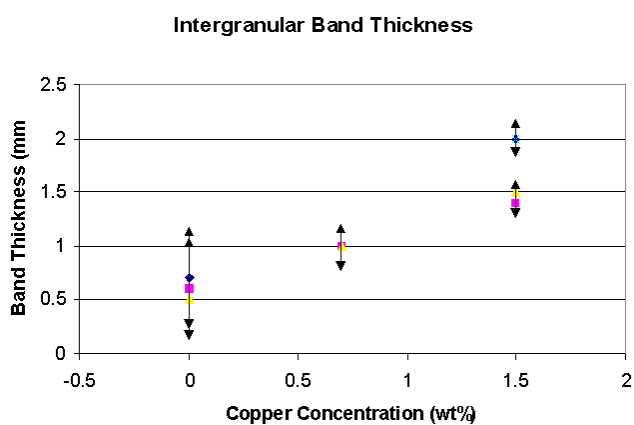


Figure 3 Plot of intergranular corrosion band thickness for experimental Al 6XXX alloys showing average penetration depth including variation during 6-10 days of polarization at $-300 \text{ mV}_{\text{SCE}}$ in 0.05M HCl.